

# An averaging method for nonlinear laminar Ekman layers

By **A. ANDERSEN**<sup>1,2†</sup>, **B. LAUTRUP**<sup>3</sup> AND **T. BOHR**<sup>1</sup>

<sup>1</sup>The Technical University of Denmark, Department of Physics,  
DK-2800 Kgs. Lyngby, Denmark

<sup>2</sup>Risø National Laboratory, Optics and Fluid Dynamics Department,  
DK-4000 Roskilde, Denmark

<sup>3</sup>The Niels Bohr Institute, Blegdamsvej 17, DK-2100 Copenhagen Ø, Denmark

(Received 22 August 2002 and in revised form 27 February 2003)

We study steady laminar Ekman boundary layers in rotating systems using an averaging method similar to the technique of von Kármán and Pohlhausen. The method allows us to explore nonlinear corrections to the standard Ekman theory even at large Rossby numbers. We consider both the standard self-similar ansatz for the velocity profile, which assumes that a single length scale describes the boundary layer structure, and a new non-self-similar ansatz in which the decay and the oscillations of the boundary layer are described by two different length scales. For both profiles we calculate the up-flow in a vortex core in solid-body rotation analytically. We compare the quantitative predictions of the model with the family of exact similarity solutions due to von Kármán and find that the results for the non-self-similar profile are in almost perfect quantitative agreement with the exact solutions and that it performs markedly better than the self-similar profile.

---

## 1. Introduction

Ekman layers are boundary layers which form in rotating systems at either free or solid boundaries, typically normal to the axis of rotation. Such boundary layers play important roles in many geophysical and technical flows, including large atmospheric vortices and source-sink flows in turbines (Lugt 1995). In the bulk, far from any walls, such flows are essentially two-dimensional with velocities mainly perpendicular to the axis of rotation. Due to the Ekman layer, however, there is also a small but important velocity component along the axis of rotation, which is referred to as either Ekman pumping or suction. The properties of Ekman layers are well-described by linear differential equations when the flow in the rotating reference system is weak compared with the background rotation, i.e. at low Rossby number. The Rossby number is defined as the characteristic value of the ratio of the nonlinear terms and the Coriolis terms in the Navier–Stokes equations in the frame of reference rotating with the background rotation rate (Batchelor 1967). At large values of the Rossby number the nonlinear terms become important, which makes it difficult to solve the governing equations and creates a need for approximate methods.

† Present address: Cornell University, Department of Theoretical and Applied Mechanics, Ithaca, NY 14853, USA.

We model the nonlinear Ekman layers at solid boundaries for flows with rotational symmetry using an averaging method similar to the technique introduced by von Kármán (1921) and Pohlhausen (1921). Owen, Pincombe & Rogers (1985) applied an averaging method to describe laminar and turbulent boundary layers in rotating fluids. They used a self-similar boundary layer profile (described by a single length scale) and focused on a particular geometry in which up-flow from the boundary layer does not occur because of the symmetry of the problem. We extend their equations to include the terms describing up-flow from the boundary layer. The self-similar profile has the same damped oscillatory structure as the solution to the linear Ekman equations but with a boundary layer thickness which depends on the local Rossby number. To investigate the applicability of the method we compare the results with the family of similarity solutions due to von Kármán (1921) for the flow above an infinite rotating disk. In this family of solutions the fluid far above the disk is in solid-body rotation with a different rotation rate to that of the disk. The results agree qualitatively, but the quantitative agreement is poor, leading, e.g., to a considerable overestimate of the Ekman pumping. We trace this discrepancy to the assumption that a self-similar ansatz for the velocity profile based on a single length scale can describe both the oscillatory and the exponential components of the boundary layer. This is correct for the linear solution but for the nonlinear case there is no basis for such an assumption. We thus introduce a non-self-similar profile which involves two length scales and show that the boundary layer structure and the up-flow for the non-self-similar profile agree almost perfectly with the family of von Kármán similarity solutions at arbitrary (positive) Rossby number.

## 2. Linear Ekman theory

We focus on the flow in a container with rotational symmetry which is rotating about its vertical axis of symmetry, and we thus apply the Navier–Stokes equations in polar coordinates written in the frame of reference co-rotating with the container. We let  $u$ ,  $v$ , and  $w$  denote the radial, the azimuthal, and the vertical velocity component, respectively. In the bulk of the fluid the flow is approximately two-dimensional, independent of the vertical coordinate  $z$  and we denote the azimuthal velocity there by  $v_0$ . At the bottom of the container there is a mismatch between the bulk velocity and the rigidly rotating solid bottom, and therefore an Ekman layer is formed (see e.g. Batchelor 1967). We assume that the vertical velocity component is small and from the vertical Navier–Stokes equation it thus follows that the effective pressure is independent of  $z$  and equal to its value in the geostrophic bulk of the fluid, i.e. far above the bottom Ekman layer. It is convenient to write the governing equations using the non-dimensional variables

$$r = L \bar{r}, \tag{2.1}$$

$$z = \sqrt{\frac{\nu}{\Omega}} \bar{z}, \tag{2.2}$$

$$u = V \bar{u}, \tag{2.3}$$

$$v = V \bar{v}, \tag{2.4}$$

$$w = \sqrt{\frac{\nu}{\Omega}} \frac{V}{L} \bar{w}, \tag{2.5}$$

where  $\nu$  is the kinematic viscosity and  $\Omega$  is the angular velocity of the container. The different scaling of  $r$  and  $z$  is introduced since the thickness of the Ekman boundary

layer is  $\sqrt{\nu/\Omega}$  in the linear approximation. In the following we drop the tilde and use only the non-dimensional variables. At small Rossby number the governing equations reduce to the following linear equations:

$$0 = \frac{1}{2} \frac{\partial^2 u}{\partial z^2} + v - v_0, \quad (2.6)$$

$$0 = \frac{1}{2} \frac{\partial^2 v}{\partial z^2} - u. \quad (2.7)$$

With the boundary conditions  $u(r, z) = v(r, z) = 0$  at  $z = 0$ ,  $u(r, z) \rightarrow 0$  as  $z \rightarrow \infty$ , and  $v(r, z) \rightarrow v_0(r)$  as  $z \rightarrow \infty$ , the solution is

$$u(r, z) = -v_0(r) e^{-z} \sin z, \quad (2.8)$$

$$v(r, z) = v_0(r) [1 - e^{-z} \cos z]. \quad (2.9)$$

The continuity equation links  $u$  and  $w$ :

$$\frac{1}{r} \frac{\partial(ru)}{\partial r} + \frac{\partial w}{\partial z} = 0, \quad (2.10)$$

and since  $w(r, z) = 0$  for  $z = 0$  we have

$$w(r, z) = \frac{1}{2r} \frac{d(rv_0)}{dr} (1 - e^{-z} [\sin z + \cos z]). \quad (2.11)$$

It follows that the vertical velocity component in the bulk of the fluid is proportional to the  $z$ -component of the vorticity there:

$$w_0 = \frac{1}{2r} \frac{d(rv_0)}{dr}. \quad (2.12)$$

Depending on the sign of  $w_0$ , this is referred to as Ekman pumping or Ekman suction. If the fluid is rotating as a solid-body with  $v_0 = r$  it follows that

$$w_0 = 1. \quad (2.13)$$

A cyclonic vortex of this kind thus generates up-flow whereas an anticyclonic vortex gives rise to down-flow. In the following we analytically calculate nonlinear corrections to (2.13) using the averaged equations.

### 3. Averaged boundary layer equations

#### 3.1. Governing equations

The linear equations (2.6) and (2.7) are only valid when the flow in the co-rotating reference system is weak and the nonlinear terms can be neglected compared to the Coriolis terms, i.e. at small Rossby number. At larger values of the Rossby number we approximate the radial and the azimuthal Navier–Stokes equations by boundary layer equations in which we neglect the derivatives with respect to  $r$  in the viscous terms:

$$Ro \left( u \frac{\partial u}{\partial r} + w \frac{\partial u}{\partial z} - \frac{v^2 - v_0^2}{r} \right) = \frac{1}{2} \frac{\partial^2 u}{\partial z^2} + v - v_0, \quad (3.1)$$

$$Ro \left( u \frac{\partial v}{\partial r} + w \frac{\partial v}{\partial z} + \frac{uv}{r} \right) = \frac{1}{2} \frac{\partial^2 v}{\partial z^2} - u, \quad (3.2)$$

where  $v(r, z) \rightarrow v_0(r)$  when  $z \rightarrow \infty$  and where we define the Rossby number

$$Ro = \frac{V}{2\Omega L}. \quad (3.3)$$

Equations (3.1) and (3.2) are used in the following as the starting point in the derivation of the averaged equations.

### 3.2. Self-similar profile

In the averaging method we make an ansatz on the  $z$ -dependence of the velocity field, i.e. on the boundary layer structure. Following Owen *et al.* (1985) we make a straightforward generalization of (2.8)–(2.9) and consider the self-similar profile

$$u(r, z) = u_0 f(z/\delta), \quad (3.4)$$

$$v(r, z) = v_0 [1 - g(z/\delta)], \quad (3.5)$$

where  $u_0$ ,  $v_0$ , and  $\delta$  are functions of  $r$ , and where

$$f(\eta) \equiv \exp(-\eta) \sin \eta, \quad (3.6)$$

$$g(\eta) \equiv \exp(-\eta) \cos \eta. \quad (3.7)$$

The term ‘self-similar’ is used here to emphasize that the profile does not depend on both  $r$  and  $z$  but only on the combination  $z/\delta(r)$ . We integrate the governing equations (3.1) and (3.2) with respect to  $z$  from zero to infinity and obtain the averaged equations

$$Ro \left( I_2 \frac{1}{r} \frac{d(r u_0^2 \delta)}{dr} + (2I_4 - I_5) \frac{v_0^2}{r} \delta \right) = -\frac{u_0}{2\delta} f'(0) - I_4 v_0 \delta, \quad (3.8)$$

$$Ro \left( (I_1 - I_3) \frac{1}{r^2} \frac{d(r^2 u_0 v_0 \delta)}{dr} - I_1 \frac{v_0}{r} \frac{d(r u_0 \delta)}{dr} \right) = \frac{v_0}{2\delta} g'(0) - I_1 u_0 \delta, \quad (3.9)$$

where the following definitions of integrals are used:

$$I_1 = \int_0^\infty d\eta f(\eta) = \frac{1}{2}, \quad I_2 = \int_0^\infty d\eta f^2(\eta) = \frac{1}{8}, \quad (3.10)$$

$$I_3 = \int_0^\infty d\eta f(\eta) g(\eta) = \frac{1}{8}, \quad I_4 = \int_0^\infty d\eta g(\eta) = \frac{1}{2}, \quad (3.11)$$

$$I_5 = \int_0^\infty d\eta g^2(\eta) = \frac{3}{8}. \quad (3.12)$$

Equations (3.8) and (3.9) are written for a general self-similar profile as defined by (3.4) and (3.5). The integrals can be evaluated as shown in (3.10)–(3.12) for the ansatz (3.6) and (3.7), and the governing equations become

$$Ro \left( \frac{1}{4r} \frac{d(r u_0^2 \delta)}{dr} + \frac{5v_0^2}{4r} \delta \right) = -\frac{u_0}{\delta} - v_0 \delta, \quad (3.13)$$

$$Ro \left( \frac{3}{4r^2} \frac{d(r^2 u_0 v_0 \delta)}{dr} - \frac{v_0}{r} \frac{d(r u_0 \delta)}{dr} \right) = -\frac{v_0}{\delta} - u_0 \delta. \quad (3.14)$$

Notice that  $w$  does not appear in the averaged equations. The flow rate,  $q$ , of the radial inflow is

$$q \equiv -2\pi r \int_0^\infty dz u = -2\pi r u_0 \int_0^\infty dz f(z/\delta) = -\pi r u_0 \delta. \quad (3.15)$$

Owen *et al.* (1985) assumed that  $q$  is independent of  $r$  and therefore the second term on the left-hand side of (3.14) is absent in their averaged azimuthal equation.

With linear velocity profiles  $u_0 = -Ar$  and  $v_0 = r$ , we find that  $\delta$  becomes independent of  $r$  and equations (3.13) and (3.14) reduce to the algebraic equations

$$Ro \left( \frac{3}{4} A^2 + \frac{5}{4} \right) = \frac{A}{\delta^2} - 1, \quad (3.16)$$

$$-Ro A = -\frac{1}{\delta^2} + A. \quad (3.17)$$

In this case we set  $V = CL$  and we thus have  $Ro = C/(2\Omega)$ . The vertical velocity component in the bulk of the fluid,  $w_0$ , is related to the radial velocity component  $u_0$  through the continuity equation (2.10):

$$w_0 = -\frac{1}{2r} \frac{d(ru_0\delta)}{dr}, \quad (3.18)$$

and thus it follows that the assumption of a linear radial velocity profile leads to

$$w_0 = \delta A. \quad (3.19)$$

By solving (3.16) and (3.17) for  $\delta$  and  $A$  it follows that the nonlinear Ekman pumping velocity is less than the linear result as the Rossby number is increased:

$$w_0 = \left[ \frac{4 + 5Ro}{(4 + Ro)(1 + Ro)^2} \right]^{1/4}. \quad (3.20)$$

At  $Ro = 0$  the right-hand side is equal to 1, in agreement with linear Ekman theory (2.13), and in the limit of infinite Rossby number the dimensional up-flow velocity  $W_0$  is independent of  $\Omega$  and equal to  $W_0 = 20^{1/4} \sqrt{\nu C} \approx 2.115 \sqrt{\nu C}$ .

### 3.3. Non-self-similar profile

As we will show in §5 the self-similar profile leads to predictions which are not in quantitative agreement with the family of exact similarity solutions due to von Kármán. We thus introduce the following non-self-similar boundary layer profile:

$$u(r, z) = -v_0 e^{-z/\delta_1} \sin(z/\delta_2), \quad (3.21)$$

$$v(r, z) = v_0 [1 - e^{-z/\delta_1} \cos(z/\delta_2)], \quad (3.22)$$

where  $v_0$ ,  $\delta_1$ , and  $\delta_2$  are functions of  $r$ . Like the self-similar profile this is a generalization of (2.8)–(2.9) but now with two length scales describing respectively the decay and the oscillations in the boundary layer structure. In this expression we have not allowed for different amplitudes on the radial and azimuthal fields. Allowing this would require another condition to close the system of equations. We have investigated the case where this other condition is the standard wall curvature compatibility condition

$$\frac{1}{2} \frac{\partial^2 u}{\partial z^2} \Big|_{z=0} = v_0 + Ro \frac{v_0^2}{r}. \quad (3.23)$$

The resulting equations are considerably more complex, and lead to no appreciable improvement in the problems that we have considered.

At low Rossby number  $\delta_1 = \delta_2 = 1$  but in general the two length scales are different. The presence of two length scales in the solution is apparent in the exact asymptotic solution at large  $z$  as shown by Bödewadt (1940) and Rogers & Lance (1960). Our ansatz has the same structure as the special asymptotic solution which also satisfies the no-slip boundary condition at  $z = 0$ . The averaged equations are in this case

$$Ro \left( \frac{1}{r} \frac{d(rv_0^2 K_2)}{dr} + \frac{v_0^2}{r} (2K_4 - K_5) \right) = \frac{v_0}{2\delta_2} - v_0 K_4, \quad (3.24)$$

$$Ro \left( \frac{1}{r^2} \frac{d(r^2 v_0^2 K_3)}{dr} - \frac{v_0 K_1}{r} \frac{d(rv_0)}{dr} \right) = -\frac{v_0}{2\delta_1} + v_0 K_1, \quad (3.25)$$

where we define

$$K_1 = 4K_3 = \frac{\delta_1^2 \delta_2}{\delta_1^2 + \delta_2^2}, \quad K_2 = \frac{\delta_1^3}{4(\delta_1^2 + \delta_2^2)}, \quad (3.26)$$

$$K_4 = \frac{\delta_1 \delta_2^2}{\delta_1^2 + \delta_2^2}, \quad K_5 = K_2 + \frac{1}{2} K_4. \quad (3.27)$$

With the linear velocity profile  $v_0 = r$ , the averaged equations reduce to

$$Ro \left( \frac{1}{2} \delta_1^2 + \frac{3}{2} \delta_2^2 \right) = \frac{\delta_1^2 + \delta_2^2}{2\delta_1 \delta_2} - \delta_2^2, \quad (3.28)$$

$$-Ro \delta_1^2 = -\frac{\delta_1^2 + \delta_2^2}{2\delta_1 \delta_2} + \delta_1^2, \quad (3.29)$$

under the assumption that  $\delta_1$  and  $\delta_2$  do not depend on  $r$ . Using the non-self-similar profile we thus predict that the nonlinear Ekman pumping velocity is reduced in the following way in comparison with the linear result

$$w_0 = \frac{[(2 + Ro)(2 + 3Ro)]^{1/4}}{\sqrt{2}(1 + Ro)}. \quad (3.30)$$

Like (3.20) the right-hand side is equal to 1 when  $Ro = 0$ , and in the limit of infinite  $Ro$  the dimensional up-flow velocity is  $W_0 = 3^{1/4} \sqrt{\nu C} \approx 1.316 \sqrt{\nu C}$ . The non-self-similar profile thus gives a weaker up-flow than the self-similar profile in the limit of large Rossby number.

#### 4. Numerical solution for source–sink vortex

Source–sink flows in a rotating cylindrical container are important examples of vortex flows controlled by Ekman layers. In this section we consider a generic source–sink vortex and assume an azimuthal velocity profile of the form

$$v_0 = \frac{1}{r} [1 - \exp(-r^2)]. \quad (4.1)$$

The velocity profile is linear when  $r \ll 1$ , and it is like a line vortex when  $r \gg 1$ . This is similar to a Rankine vortex, and the profile is thus like a smooth Rankine vortex with a soft transition between the vortex core and the outside velocity field. It follows

by definition that the  $z$ -component of vorticity has a Gaussian profile and in linear Ekman theory we thus predict that the up-flow is

$$w_0 = \exp(-r^2). \quad (4.2)$$

The vertical velocity component in the bulk of the fluid,  $w_0$ , is related to  $q$  through the continuity equation:

$$w_0 = \frac{1}{2\pi r} \frac{dq}{dr}, \quad (4.3)$$

and integration gives the following expression for  $q$  in terms of  $w_0$ :

$$q(r) = Q - 2\pi \int_r^\infty dx w_0(x)x, \quad (4.4)$$

where  $Q$  is defined as the limit value of  $q$  for large  $r$ . At  $r \gg 1$  linear Ekman theory is valid since the local Rossby number there is small, and the circulation of the vortex is thus linked to the flow rate which leads to  $Q = \pi$ .

To obtain numerical solutions for the self-similar profile we eliminate the boundary layer thickness  $\delta$  in the averaged equations (3.13) and (3.14) and use  $u_0$ ,  $v_0$ , and  $q$  as the dependent variables. We write the equations in the following form, assuming the azimuthal velocity component  $v_0$  to be known:

$$u'_0 = -\frac{3u_0v'_0}{v_0} - \frac{3u_0}{r} - \frac{5v_0^2}{ru_0} - \frac{4}{Ro} \left( \frac{2\pi^2 r^2 u_0^2}{q^2} + \frac{u_0}{v_0} + \frac{v_0}{u_0} \right), \quad (4.5)$$

$$q' = \frac{3qv'_0}{v_0} + \frac{3q}{r} + \frac{4}{Ro} \left( \frac{\pi^2 r^2 u_0}{q} + \frac{q}{v_0} \right), \quad (4.6)$$

and supplement the equations by boundary conditions at large  $r = R$ :

$$u_0(R) = -\frac{1}{R} \quad (4.7)$$

$$q(R) = \pi. \quad (4.8)$$

To solve the equations for the non-self-similar profile numerically we use the functions  $\alpha \equiv K_1$  and  $\beta \equiv \delta_1/\delta_2$  and rewrite equations (3.24) and (3.25) in terms of them as

$$\alpha' = \frac{2}{v_0} \left[ \left( v'_0 + \frac{v_0}{r} + \frac{2}{Ro} \right) \alpha - \frac{1}{Ro \delta_1} \right], \quad (4.9)$$

$$\beta' = -\frac{2}{\alpha v_0} \left[ \left( 2v'_0 + \frac{v_0}{r} + \frac{2}{Ro} \right) \alpha \beta + \left( \frac{3v_0}{r} + \frac{2}{Ro} \right) \frac{\alpha}{\beta} - \frac{2}{Ro \delta_2} \right], \quad (4.10)$$

where  $\delta_1$  and  $\delta_2$  are expressed in terms of  $\alpha$  and  $\beta$ . We supplement the equations by the following boundary conditions at large  $r = R$ :

$$\alpha(R) = \frac{1}{2} \quad (4.11)$$

$$\beta(R) = 1. \quad (4.12)$$

Figure 1 shows the solution for  $v_0$ ,  $u_0$ ,  $w_0$ , and  $\delta$  with a central Rossby number of 1. At large values of  $r$  the solution is well-described by the linear theory, whereas the boundary layer thickness decreases closer to the vortex centre compared to the constant linear Ekman layer thickness. The central up-flow velocities are described quantitatively by (3.20) and (3.30) with  $Ro = 1$ .

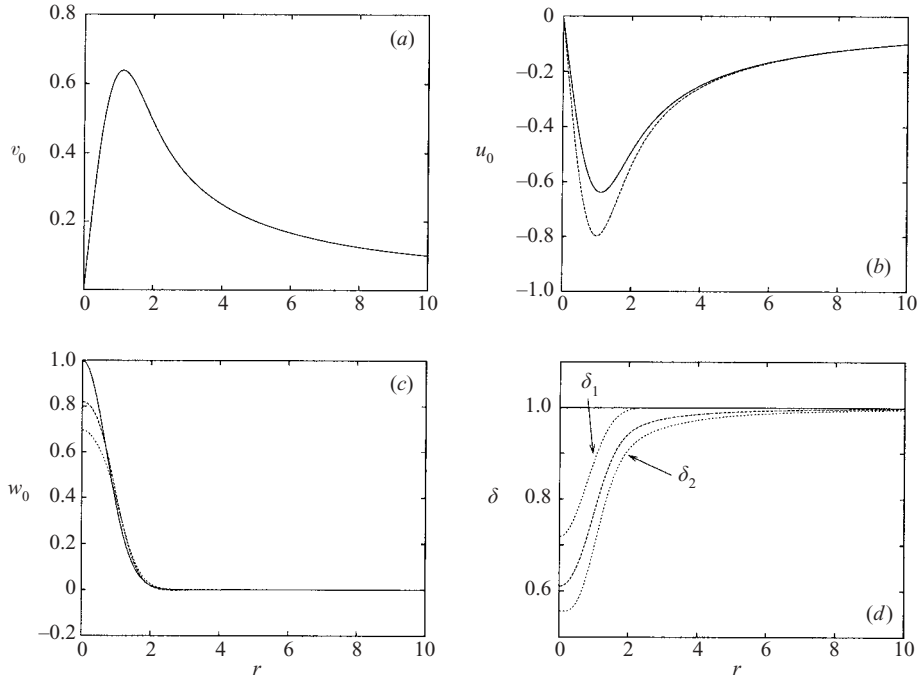


FIGURE 1. Numerical solution of the averaged equations for the source–sink vortex. (a) The assumed azimuthal velocity  $v_0$ , (b) the radial velocity  $u_0$ , (c) the vertical velocity  $w_0$ , and (d) the boundary layer thickness  $\delta$  all computed at a central Rossby number of 1. The solid curves show the linear theory, the dashed curves the result obtained with the self-similar profile, and the dotted curves the result obtained with the non-self-similar profile. In (b) the solid and the dotted curves are identical by assumption and thus only the solid curve is shown.

## 5. The family of similarity solutions by von Kármán

In this section we investigate the applicability of the self-similar and the non-self-similar boundary layer profiles by comparing them to the family of similarity solution due to von Kármán (1921). This family of solutions describes the flow above a flat rotating disk of infinite extent with the fluid infinitely high above the disk in solid-body rotation with a different rotation rate to that of the disk. The similarity assumption was introduced by von Kármán (1921) in the special case in which the fluid is not rotating far above the rotating disk, and the general family of solutions was investigated numerically by Rogers & Lance (1960). The similarity solutions are obtained with the following ansatz for the velocity field:

$$u(r, z) = r F(z), \quad (5.1)$$

$$v(r, z) = r G(z), \quad (5.2)$$

$$w(r, z) = H(z). \quad (5.3)$$

With this ansatz the Navier–Stokes equations reduce to a set of ordinary differential equations for  $F$ ,  $G$ , and  $H$ . The Navier–Stokes equations and the continuity equation in the co-rotating frame of reference become

$$Ro (F^2 + H F' - G^2 + 1) = \frac{1}{2} F'' + G - 1, \quad (5.4)$$

$$Ro (2 F G + H G') = \frac{1}{2} G'' - F, \quad (5.5)$$



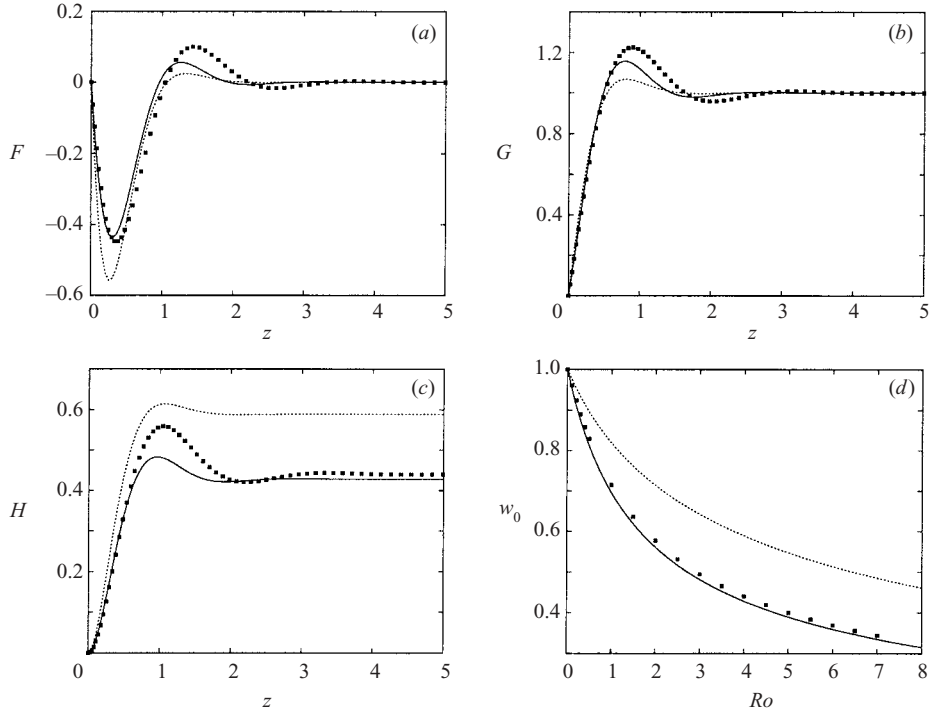


FIGURE 2. Solutions of the von Kármán similarity flows. (a–c) the boundary layer structure of  $u$ ,  $v$ , and  $w$  at  $Ro = 4$ , and (d) the ratio between the nonlinear up-flow velocity and the result from linear Ekman theory as function of  $Ro$ . The symbols show the numerical solution of (5.4)–(5.7), the dotted curves the result from (3.16) and (3.17) obtained with the self-similar profile, and the solid curves the result from (3.28) and (3.29) obtained with the non-self-similar profile.

$$Ro H H' = -P' + \frac{1}{2} H'', \quad (5.6)$$

$$2F + H' = 0, \quad (5.7)$$

which are to be supplemented by the five boundary conditions

$$F(0) = 0, \quad F(\infty) = 0, \quad (5.8)$$

$$G(0) = 0, \quad G(\infty) = 1, \quad (5.9)$$

$$H(0) = 0. \quad (5.10)$$

In the original problem considered by von Kármán the azimuthal velocity goes to zero far above the disk in the laboratory frame corresponding to  $C = -\Omega$ .

Figure 2 shows numerical solutions (symbols) of equations (5.4)–(5.7) together with results of the averaging method with the self-similar profile (dotted curves) and the non-self-similar profile (solid curves). The solution with the non-self-similar profile has  $\delta_1 \geq \delta_2$  and it captures the damped oscillatory structure of the exact solution at  $Ro = 4$  markedly better than the self-similar profile. This is particularly evident for the vertical velocity component shown in figure 2(d) for Rossby numbers between 0 and 8. The asymptotic behaviour of the exact solution in the limit of infinite Rossby number was described by Bödewadt (1940) who found that  $W_0 = 1.349 \sqrt{\nu C}$ . The prediction,  $W_0 \approx 1.316 \sqrt{\nu C}$ , obtained using the non-self-similar profile agrees well

with this result whereas the method using the self-similar profile overestimates the up-flow velocity,  $W_0 \approx 2.115 \sqrt{\nu C}$ .

## 6. Conclusions

We have analysed two methods based on averaging for computing the structure of nonlinear Ekman layers. We find that a non-self-similar velocity profile with separate length scales for the decay and the oscillations, respectively, gives very accurate predictions. We believe that this method will be useful for many important flow configurations and hope that it will be compared to accurate measurements of the up-flow in well-controlled laboratory experiments and ideally with velocity measurements resolving the Ekman layer structure.

We thank Jens Juul Rasmussen and Bjarne Stenum for many valuable discussions.

## REFERENCES

- BATCHELOR, G. K. 1967 *An Introduction to Fluid Dynamics*. Cambridge University Press.
- BÖDEWADT, U. T. 1940 Die Drehströmung über festem Grunde. *Z. Angew. Math. Mech.* **20**, 241–253.
- KÁRMÁN, T. VON 1921 Über laminare und turbulente Reibung. *Z. Angew. Math. Mech.* **1**, 233–252.
- LUGT, H. J. 1995 *Vortex Flow in Nature and Technology*. Krieger.
- OWEN, J. M., PINCOMBE, J. R. & ROGERS, R. H. 1985 Source-sink flow inside a rotating cylindrical cavity. *J. Fluid Mech.* **155**, 233–265.
- POHLHAUSEN, K. 1921 Zur näherungsweise Integration der Differentialgleichung der laminaren Grenzschicht. *Z. Angew. Math. Mech.* **1**, 252–268.
- ROGERS, M. H. & LANCE, G. N. 1960 The rotationally symmetric flow of a viscous fluid in the presence of an infinite rotating disk. *J. Fluid Mech.* **7**, 617–631.